The homeodomain protein Vax1 is required for axon guidance and major tract formation in the developing forebrain

Stefano Bertuzzi,[1] Robert Hindges,[1] Stina H. Mui,[1,2] Dennis D.M. O'Leary,[1] and Greg Lemke[1,3]

[1]Molecular Neurobiology Laboratory, The Salk Institute for Biological Studies, La Jolla, California 92037 USA; [2]Department of Neurosciences, University of California at San Diego, La Jolla, California 92093 USA

The homeodomain protein Vax1 is expressed in a highly circumscribed set of cells at the ventral anterior midline of the embryonic CNS. These cells populate the choroid fissure of the optic disk, the body of the optic stalk and nerve, the optic chiasm and ventral diencephalon, and the anterior midline zones that abut developing commissural tracts. We have generated mutant mice that lack Vax1. In these mice (1) the optic disks fail to close, leading to coloboma and loss of the eye-nerve boundary; (2) optic nerve glia fail to associate with and appear to repulse ingrowing retinal axons, resulting in a fascicle of axons that are completely segregated from optic nerve astrocytes; (3) retinal axons fail to penetrate the brain in significant numbers and fail to form an optic chiasm; and (4) axons in multiple commissural tracts of the anterior CNS, including the corpus callosum and the hippocampal and anterior commissures, fail to cross the midline. These axon guidance defects do not result from the death of normally Vax1+ midline cells but, instead, correlate with markedly diminished expression of attractive guidance cues in these cells. Vax1 therefore regulates the guidance properties of a set of anterior midline cells that orchestrate axon trajectories in the developing mammalian forebrain.

Glial cells have essential axon guidance roles in the developing *Drosophila* CNS, notably in the control of pathway choice as axonal growth cones encounter the midline glia of the ventral nerve cord (Jacobs and Goodman 1989; Klambt et al. 1991; Hummel et al. 1997). Several of the midline glial genes that underly this control have been identified and cloned (Rothberg et al. 1990; Tear et al. 1996; Kidd et al. 1999), and have been found to encode chemoattractants such as the Netrins (Mitchell et al. 1996; Winberg et al. 1998), dual-function chemorepellents such as Slit (Battye et al. 1999; Kidd et al. 1999), and proteins such as Commissureless, which appear to modulate the ability of growth cones to respond to midline guidance cues (Tear et al. 1996). Although the molecular details of signal presentation by midline glia and their interpretation by axonal growth cones are still being worked out, the axon guidance defects seen in mutants of the *slit*, *roundabout*, *netrin A* and *B*, *commissureless*, and *frazzled* genes clearly demonstrate that growth cone navigation at the ventral midline is a combinatorial function of attractive and repulsive guidance cues provided by midline glia, and of the differential ability of commissural and longitudinal axons to respond to these cues as their growth cones approach and cross the midline (Zinn and Sun 1999).

The extent to which vertebrate glia may have similar axon guidance roles during neural development is less well understood in molecular terms, although the pioneering position and intimate axonal association of early glia at CNS midline structures such as the optic chiasm and corpus callosum has prompted considerable conjecture in this regard (Silver 1993; Marcus et al. 1995; Mason and Stretavan 1997). Detailed observations of axonal projections into and through the developing mouse optic chiasm, for example, have suggested that age-dependent variations in the cues provided by morphologically and molecularly distinct populations of midline glial cells in the ventral diencephalon control the development and interhemispheric decussation of axons projecting from the retina to the superior colliculus (Marcus and Mason 1995; Marcus et al. 1995, 1999; Wang et al. 1995). Similarly, studies in the embryonic cat, rat, and mouse brain

[3]Corresponding author.
E-MAIL lemke@salk.edu; FAX (858) 455-6138.

have suggested that early midline astroglia provide the substrate for the formation of commissural fiber tracts, such as the corpus callosum and the anterior and hippocampal commissures, which cross the midline and thereby connect the two hemispheres of the developing mammalian forebrain (Silver and Ogawa 1983; Silver 1993; Silver et al. 1993). Netrin-1 (Serafini et al. 1996; Livesey and Hunt 1997) and mammalian Slit proteins (Li et al. 1999; Nguyen Ba-Charvet 1999; Wu et al. 1999) are expressed in regions populated by these midline glia.

The important issue of upstream transcriptional regulation of midline differentiation, particularly with regard to the regulated expression of Netrins, Slits, or other guidance cues, has thus far received limited attention. The ETS domain transcription factor Pointed (Klambt 1993), the POU domain protein Drifter (Anderson et al. 1995), and the SOX-related transcription factor Dichaete (Soriano and Russell 1998) are all expressed in early midline glia in *Drosophila*, and are known to be required for their normal differentiation, as evidenced by fused commissures in the ventral nerve cords of *pointed*, *drifter*, and *Dichaete* mutants. However, the molecular basis of the axon guidance phenotypes seen in these mutants is largely uncharacterized with respect to the expression of guidance cues. Mutational analyses of one vertebrate gene product expressed by glial cells of the developing optic nerve—the Paired domain transcription factor Pax2 (Dressler et al. 1990; Torres et al. 1996) and its zebrafish homolog Pax2.1 [*No isthmus* (*Noi*)] (Macdonald et al. 1997; Pfeffer et al. 1998)—have demonstrated that this protein is essential for normal axon growth within the nerve. An important guidance cue that is lost in the optic nerve astroglia of the *Noi* mutants is Netrin-1 (Macdonald et al. 1997). However, Pax2 is not expressed by the specialized glia that appear to guide midline axon crossing in the brain proper, for example, those at the corpus callosum and the anterior commissure (Torres et al. 1996; Macdonald et al. 1997; see Fig. 2, below), and therefore cannot function as a direct regulator of glial differentiation at these critical midline positions.

Recently, a new candidate regulator of midline differentiation in vertebrates—a homeodomain transcription factor designated Vax1—has been identified (Hallonet et al. 1998). The amino acid sequence of the homeodomain of this protein defines a new homeodomain subfamily whose members are most similar to the *Drosophila* protein Empty spiracles (Ems) and its related vertebrate homologs Emx-1 and Emx-2 (Hallonet et al. 1998; S. Bertuzzi and G. Lemke, unpubl.). In vivo, expression of *Vax 1* is highly restricted to ventral anterior regions of the developing CNS (Hallonet et al. 1998; see Fig. 2, below), including the glial precursor cells of the optic stalk and their descendent astrocytes of the optic nerve, and regions containing the glia that are thought to guide the formation of midline commissural tracts. We cloned *Vax1* from cultured rat Schwann cells, the principal glial cells of the vertebrate peripheral nervous system, although we have not observed Vax1 expression in any developing Schwann cell population in vivo. In cell culture, the expression of *Vax1* mRNA is highly restricted

to glial cells and glial cell lines (S. Bertuzzi and G. Lemke, unpubl.).

We have investigated the function of Vax1 by engineering loss-of-function mutations in the mouse. Among several possibilities, we sought to determine whether Vax1 (1) regulates the development, proliferation, or survival of the midline cells in which it is expressed; (2) functions to pattern the developing forebrain along the medial–lateral, dorsal–ventral, or anterior–posterior axes; or (3) controls the axon guidance properties of midline cells through upstream regulation of the genes encoding guidance cues. We find that *Vax1* mutants exhibit no obvious deficiencies in midline cell number and, at most, modest defects in axial patterning at the midline. In contrast, these mutants display profound defects in axon guidance in the optic nerve and across the ventral anterior midline of the forebrain, many of which may be accounted for by the loss of appropriate axon guidance cues at the midline.

Results

Targeting the Vax1 locus

We replaced the wild-type *Vax1* gene with a deleted gene by homologous recombination in mouse embryonic stem (ES) cells (Fig. 1), and used these ES cells to generate mice that lack *Vax1*, all by standard protocols (see Materials and Methods). The targeting vector for *Vax1* inactivation (Fig. 1A) deletes a 2.2-kb *Bam*HI segment of DNA that contains exons encoding the initiator ATG together with the first 166 amino-terminal residues of the protein, including the first 46 amino acids of the 60-residue homeodomain (predicted α helices 1 and 2). Amino acids equivalent to these latter residues are essential for the function of all known homeodomain transcription factors. In addition, mice carrying two copies of the diagrammed mutation do not express detectable *Vax1* mRNA (Fig. 1C). For these reasons, the *Vax1$^{-/-}$* mice described below almost certainly correspond to complete loss-of-function mutants.

Defects in axon guidance and glial interaction in the Vax1$^{-/-}$ optic stalk and nerve

Vax1 mRNA is first detected in the mouse embryo at embryonic day (E)8, in the anterior neural ridge and adjacent ectoderm (Hallonet et al. 1998; S. Bertuzzi and G. Lemke, unpubl.). By E10.5, this expression coalesces into the optic disks and optic stalks, the olfactory placodes, and the extreme rostral end of the neural tube (Fig. 2A). *Vax1* persists in derivatives of the former and latter domains into late embryogenesis, by which time expression is prominent in glial cells of the optic nerve and in cells of the rostral diencephalon (presumptive hypothalamus) (Fig. 2B). In the optic stalk, Vax1 is unambiguously the product of glial cell precursors, because the only neural cells that develop in situ from this segment of the neuroepithelium are the astrocytes that will populate the body of the mature optic nerve; the oligodendrocytes

Figure 1. Inactivation of the mouse *Vax1* gene. (*A*) Structure of the mouse *Vax1* gene, the targeting vector for inactivation, and the recombined allele. Sequences that encode the Vax1 homeodomain are contained in the second and third exons diagrammed, and are indicated in black. The first diagrammed exon contains the *Vax1* initiator ATG. The first and second exons are deleted and replaced with a G418 resistance cassette (*neo*) in the mutant allele, and a thymidine kinase cassette (*tk*) was used to select against nonhomologous recombinants (see Materials and Methods). The positions of the 5′ and 3′ probes used to assess homologous recombination of the left and right arms are indicated. (B) *Bam*HI; (H) *Hin*dIII; (S) *Sac*I. (*B*) Southern blot of *Hin*dIII-digested genomic DNA from wild-type (+/+), heterozygous mutant (+/−), and homozygous mutant (−/−) mice, hybridized with the 3′ probe indicated in *A*. (*C*) Lack of *Vax1* transcript in the subventricular zone of the ventral diencephalon of E13.5 mutant mice (−/−), as detected by in situ hybridization (see Material and Methods).
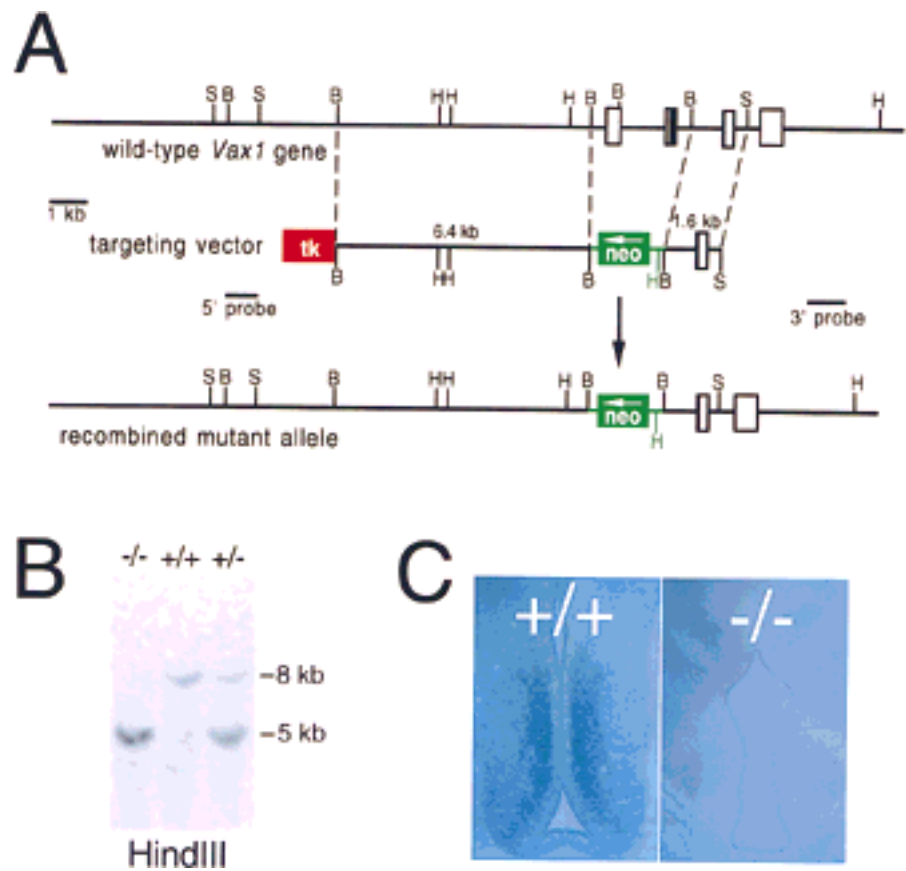
that myelinate the axons of the mature nerve develop from precursors that migrate into the nerve late in embryogenesis (beginning at E15) from germinal centers in the brain proper (Small et al. 1987; Raff 1989; Ono et al. 1997; Mi and Barres 1999). The prominent presence of *Vax1* in the presumptive hypothalamus is a feature that distinguishes this gene from *Pax2* in terms of both expression (Fig. 2B,C) and mutant phenotype (see below).

Loss of *Vax1* from the glial precursors of the optic stalk leads to obvious perturbations in retinal ganglion cell (RGC) axonogenesis and axon–glial association (Fig.

3). By E13.5, wild-type RGC axons have extended through the stalk and been invested extensively by proliferating glial precursors (Fig. 3A). Normal numbers of axons are also present in the optic stalk by E13.5 in *Vax1*$^{-/-}$ mutants; however, their growth is invariably constrained to a restricted cross-segment of the mutant stalk, from which the glial precursors are entirely excluded (Fig. 3B). These precursors normally give rise to the optic nerve astrocytes that, by late embryogenesis, are intimately associated with all RGC axons in wild-type mice (Fig. 3C); in the mutants, however, RGC axons

Figure 2. *Vax1* and *Pax2* mRNA expression in the developing brain. (*A*) *Vax1* mRNA in an E10.5 mouse embryo, detected by whole-mount in situ hybridization, is evident in the optic stalk (os, bracket), optic disk (od), olfactory pit (op), and lamina terminalis (lt). The position of the neural retina, which does not express *Vax1*, is indicated by the circle. The surface boundaries of the telencephalon (tl), midbrain (mb), and isthmus (is) are indicated by the broken lines. The CNS midline is indicated by the solid white line in this and subsequent panels. (*B*) *Vax1* mRNA (^{33}P-radiolabeled in situ), in a frontal section through the CNS of an E18.5 embryo, is expressed by the glial cells

of the two optic nerves (on, arrows) and by midline cells at the optic chiasm (oc) and in the hypothalamus (ht). Note that there is high *Vax1* expression at the junction between the optic nerve and the hypothalamus, and little *Vax1* mRNA in the ventricular zone immediately adjacent to the third ventricle. (*C*) *Pax2* mRNA, in a frontal section adjacent to that of *B*, is evident in the same optic nerve cells (on, arrows) that express *Vax1*, but not at the optic chiasm or in the hypothalamus. Scale bars, 100 μm.
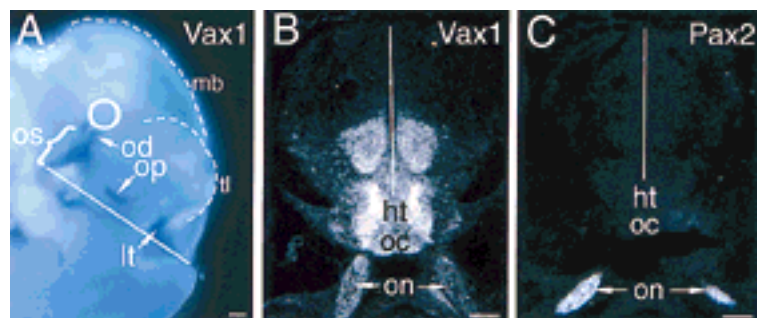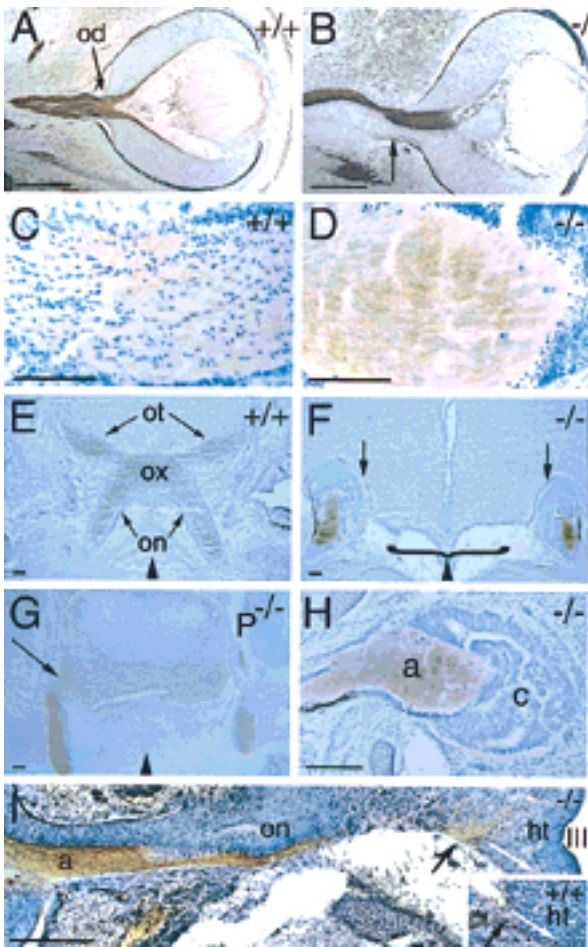
Figure 3. Defects in RGC axon pathfinding in *Vax1* mutants. (*A*) Frontal section through an E13.5 wild-type eye (facing *right*). Retinal ganglion cell axons in the optic nerve (brown) are visualized with an antibody to L1. The optic disc (od) is indicated by the arrow. (*B*) Section through an E13.5 *Vax1* mutant eye, similar to that in *A*. L1$^+$ axons fasciculate in one restricted domain of the developing optic nerve, completely avoiding the *Vax1$^{-/-}$* glial precursors of the nerve. Note that there is no longer a well-defined border between the eye and the optic nerve (apparent in *A*) and that aberrant retinal pigment epithelial cells are present at the periphery of the nerve (arrow). (*C*) High-power view of an E18.5 wild-type optic nerve, showing glial cells (toluidine blue stained, dark blue nuclei) interspersed among and regularly associating with L1$^+$ retinal axons (light brown). (*D*) Similar section to that in *C*, but in a *Vax1$^{-/-}$* optic nerve. Naked L1$^+$ axons entirely avoid and displace the glial and retinal cells of the nerve. (*E*) L1$^+$ RGC axons entering the wild-type E18.5 brain in the hypothalamus and crossing to the contralateral side of the brain at the optic chiasm (ox). The optic nerves (on) and the optic tract (ot) are indicated. (*F*) L1$^+$ retinal axons in *Vax1* mutants (also at E18.5) do not form an optic chiasm and moreover, do not penetrate the brain but, instead, terminate in encapsulated bundles. The empty space beneath the floor of the hypothalamus is contiguous with the nasal cavity and is due to the cleft palate routinely seen in *Vax1$^{-/-}$* mice (bracket). Arrows indicate the pronounced cellular barrier separating the cap of RGC axons and the brain proper. (*G*) Frontal section through the hypothalamus of E18.5 *Pax2$^{-/-}$* mouse embryo. Unlike in the *Vax1* mutant mice, retinal axons, identified by L1 staining, readily penetrate the brain (arrow), even though the *Pax2* mutants lack an organized optic chiasm. Compare the difference at the insertion points (arrows) of the optic nerves between *Vax1* mutants (*F*) and *Pax2* mutants (*G*). (*H*) High-power image of the E18.5 *Vax1* mutant cell cap, formed by optic nerve astrocyte precursors and displaced retinal cells, which encapsulate the RGC axons (a). At this stage, the thick cell cap (c) is a physical barrier preventing RGC axons from contact with the base of the brain. Note the presence of dark retinal pigment epithelial cells at the lower periphery of the distal end of the stunted optic nerve. (*I*) Tracing of the pioneer RGC axons that reach the hypothalamus in *Vax1* mutants (−/−) and in normal mice (+/+, *inset*) at E13.0. As shown in *B*, axons (a) and glial cells are separated in the optic nerve (on). Note that at this stage the cell cap at the distal end of the mutant optic nerve is not yet formed. As RGC axons reach the hypothalamus (ht), they splay out at the insertion point (black arrow), failing to fasciculate or to take the normal ventral pathway (white arrows in both montage and inset) toward the optic chiasm below the third ventricle (III). Black triangles at the *bottom* of *E–G* indicate the position of the midline. Scale bars, 100 µm.

are naked and devoid of astrocytes, which are displaced to the periphery of the nerve (Fig. 3D). The particular geometric segregation of axons and glia varies from mutant nerve to nerve, in that bundles of bare axons are sometimes observed in the center of mutant nerves and are in other instances displaced to eccentric dorsal–ventral or nasal–temporal locations. In all cases, however, the axons are virtually devoid of associated optic nerve cells (Fig. 3D).

Optic stalk glial cells are not apparently lost as a consequence of mutation; there are roughly equal numbers of nuclei per optic stalk in wild-type and *Vax1* mutant embryos at E11.5 (112 cells/10^4 µm^2 field in a wild-type longitudinal section vs. 106 cells/10^4 µm^2 field in an equivalent mutant section), and there is no measurable increase in the incidence of apoptosis in the mutants as assessed by TUNEL staining at E11.5, E13, and E18.5 (data not shown). In addition, the precursors of the stalk and nerve retain expression of *Pax2* mRNA and protein and *BF1* mRNA (see Fig. 7A,B, below), which are established markers for these cells (Torres et al. 1996; Mac-

donald et al. 1997; Shimamura and Rubenstein 1997; Otteson et al. 1998; Marcus et al. 1999).

Vax1$^{-/-}$ RGC axons fail to enter the brain

A second axon guidance phenotype becomes dramatically apparent as RGC axons approach the ventral diencephalon in the region of the presumptive hypothalamus, the site at which they normally enter the brain. This region is also an area of high *Vax1* expression (Fig. 2B), which overlaps with optic chiasm and chiasm–proximal markers such as RC2 and SSEA1 (see below). *Pax2*, although present in all mouse optic stalk cells after E12.5 (Otteson et al. 1998), is notably absent from the developing hypothalamus (Fig. 2C). The Vax1$^+$ cells at the midline of the ventral diencephalon may be glial precursors, but this has yet to be established. By E18.5, wild-type RGC axons, visualized by an antibody to the cell adhesion molecule L1 (Bartsch et al. 1989), have penetrated the brain at this site and crossed at the optic chiasm to form the well-known X-shaped retinal projec-

tion apparent in frontal sections (Fig. 3E). In *Vax1* mutants, this projection is completely absent. RGC axons fail to penetrate the hypothalamus in significant numbers, and, instead, pile up in large, encapsulated light-bulb-shaped whorls that are physically isolated from the brain proper (Fig. 3F). These capped bundles are formed at the distal ends of the optic nerve from E14.5 through E18.5 as an increasing number of proliferating Pax2$^+$ optic nerve glia and ingrowing Pax6$^+$ retinal cells (see below) are displaced laterally. However, when the RGC axons initially reach the base of the brain, the caps are not present, and there is no obvious cellular or physical barrier to their penetration of the brain. As illustrated in the E13 montage of Figure 3I, these axons fail to fasciculate and extend toward the midline of the hypothalamus (Fig. 3I, inset), where they normally form the optic chiasm; instead, they appear to simply stall and then splay out at their normal entry point in the ventral diencephalon, as if responding to a chemical rather than a physical barrier. The basic size, shape, cellular density, and histology of the developing hypothalamus are not obviously altered in the *Vax1* mutants, nor is its early dorsal–ventral or medial–lateral axial patterning affected (see Fig. 7, below).

The hypothalamic axon guidance defects seen in the *Vax1* mutants are distinct from those evident in *Pax2*$^{-/-}$ mice or *Noi (Pax2.1)* mutant zebrafish, in that RGC axons in these *Pax2* mutants readily enter the brain (Torres et al. 1996; MacDonald et al. 1997; Fig. 3G,H). The far more severe phenotype seen in the *Vax1*$^{-/-}$ mice, in which RGC axons fail to penetrate the brain and instead terminate in large whorls at the base of the hypothalamus (Fig. 3H) is consistent with the fact that *Vax1* is expressed at the midline of the developing hypothalamus, exactly where the optic nerve connects to the brain, whereas *Pax2* is not (Fig. 2B,C). In keeping with these differences in mutant phenotype, we have found that *Vax1* is normally expressed in the ventral diencephalon of mouse *Pax2* mutants (data not shown).

Coloboma in Vax1 *mutants*

From their earliest stages of development, the eyes of *Vax1*$^{-/-}$ homozygotes display coloboma—a failure of the eye to close at the choroid fissure (Fig. 4A), in which *Vax1* expression in wild-type embryos is prominent (Hallonet et al. 1998). This coloboma persists throughout the life of the mutants. Nearly all *Vax1*$^{-/-}$ mice die on the first day after birth (see below), but rare individuals (~6% of the mutants) can survive for up to 2 weeks, and coloboma persists in these animals (Fig. 4B). *Pax2* is also expressed at high levels in the optic disk, and *Pax2*$^{-/-}$ mice also display coloboma (Torres et al. 1996). Similarly, mutations in the human *PAX2* gene account for a set of inherited colobomas that are associated with renal anomalies (Sanyanusin et al. 1995). As most instances of isolated coloboma in humans are not linked to the *PAX2* gene (Cunliffe et al. 1998), it is very possible that a subset of these disorders are caused by mutations in the human homolog of the mouse *Vax1* gene. As in other instances
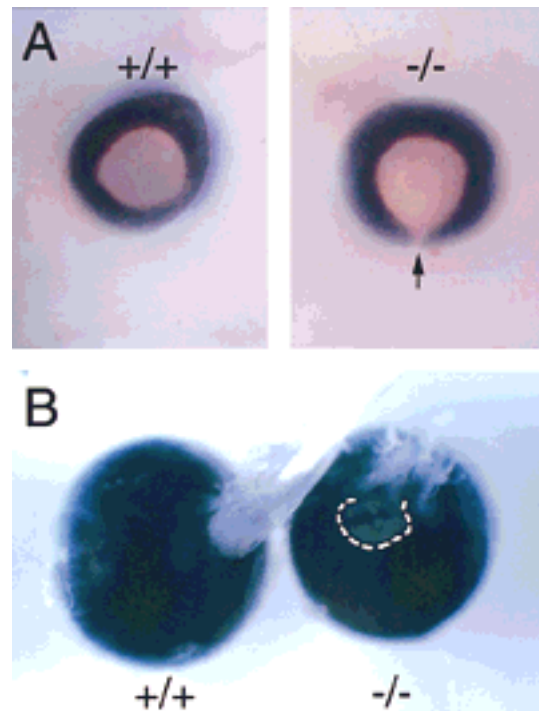

Figure 4. Homozygous *Vax1* mutant mice show bilateral coloboma and disruption of the eye/optic nerve boundary. (*A*) Coloboma is evident at the pigmented back of an E13 mutant eye (arrow in –/–), due to the failure of the optic fissure to close. (*B*) Persistence of coloboma (broken line), together with poorly organized retinal axons in the optic nerve, in a dissected P12 mutant eye (–/–) with attached disordered nerve, as compared with the closed eye and well-formed optic nerve evident in P12 wild type (+/+).

of coloboma (Torres et al. 1996; Macdonald et al. 1997), the failure of the optic disk to close disrupts the eye/nerve boundary and results in an unsealed opening at the back of the eye through which retinal cells aberrantly migrate into the developing optic nerve (Figs. 2F and 8F, below). We have frequently observed cases in which the periphery of nearly the entire length of the *Vax1* mutant nerve is pigmented by cells of the retinal pigment epithelium. In addition, Pax6$^+$ cells, which are normally confined to the retina, are readily detected in the nerve, and by late embryogenesis, constitute a large fraction of the cells that encapsulate the stalled RGC axons at the base of the hypothalamus (see below).

Neonatal death of Vax1$^{-/-}$ *mice*

Although we have not determined why most *Vax1* mutants die at birth, their immediate death may be due to the presence of a cleft palate, which is fully penetrant but is seen in varying degrees of severity among homozygous individuals (see, e.g., the open cavity at the base of the brain in Fig. 3F); severe cleft palate is generally a lethal phenotype in mice (Orioli et al. 1996). This developmental defect is almost always manifest in the secondary palate at the back of the oral cavity, which, as a

consequence, is contiguous with the nasal sinuses. The observed cleft palate may be due to developmental failures associated with the transient expression of *Vax1* in the first branchial arch (Hallonet et al. 1998). Its presence is of particular interest with regard to parallels between the *Vax1* mutants and double-mutant mice in which the genes encoding the receptor tyrosine kinases EphB2 and EphB3 are both inactivated (see below).

Fluorescent visualization of RGC afferents in Vax1$^{-/-}$ mice

The dramatic failure in RGC axon penetration of the brain in the *Vax1* mutants prompted us to examine this failure in greater detail, by fluorescently labeling these axons, through injection of the lipophilic axon tracer 1,1′-dioctodecyl-3,3,3′,3′-tetramethyl-indocarbocyanin perchlorate (DiI) into the retinae of both wild-type and mutant mice, at E16 in utero and on the day of birth (see Materials and Methods). These studies confirmed the failure of RGC axons to penetrate the brain at the base of the hypothalamus, to reach the chiasm at the midline, to cross contralaterally, or to make a stereotypical ipsilateral projection in the *Vax1* mutants (Fig. 5A–D). Instead, an analysis through successively more caudal coronal sections revealed that a small subset of *Vax1*$^{-/-}$ RGC axons escape from the knot-like whorls evident in Figure 3F and project ipsilaterally through regions of the preoptic area that are normally *Vax1* negative; that is, through regions that are lateral to the *Vax1* expression domains in Figure 2B. We speculate that these rare escapers might represent the first RGC axons to extend through the optic stalk in development. The few *Vax1*$^{-/-}$ RGC axons that escape the knot are nonetheless completely blocked from crossing the midline and project exclusively to ipsilateral visual areas (Fig. 5G,H), in marked contrast to wild-type axons, 95% of which in the mouse cross at the chiasm and project to the contralateral side of the brain (Fig. 5E,F).

Vax1$^{-/-}$ axons fail to cross the anterior midline

By mid-embryogenesis, expression of *Vax1* mRNA at the midline is detected adjacent to a number of forebrain interhemispheric fiber tracts. For example, expression is detected adjacent to the lateral ventricles, and in the septum adjacent and immediately ventral to the developing corpus callosum (Fig. 6A,B; Hallonet et al. 1998). The failure of axons to enter the brain at the midline of the rostral hypothalamus in the *Vax1* mutants prompted us to examine axon pathways in these anterior commissural axon tracts. We found that loss of *Vax1* in these anterior midline regions similarly leads to a complete loss of interhemispheric connections in the mutant forebrain. *Vax1*$^{-/-}$ mice, for example, lack a corpus callosum connecting the two cortical hemispheres (Fig. 6C,E). Instead, axons that would normally cross the midline in this thick tract terminate in large whorls of stunted axons that are deflected from the midline (asterisk in Fig. 6E). These so-called Probst bundles (Probst 1901) are
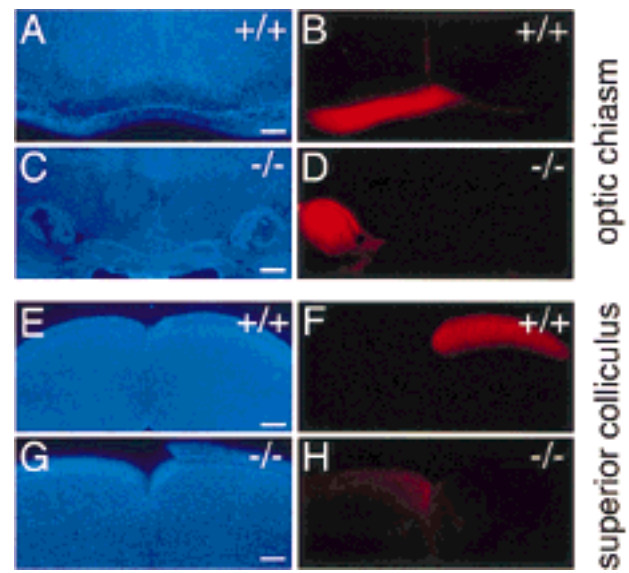

Figure 5. Growth of retinal ganglion cell axons into the brains of newborn wild-type (+/+) and *Vax1* mutant (−/−) mice. The right eyes of newborn mice were completely filled with DiI to label the axons of all RGC neurons projecting from the right retina, and mice were analyzed 1 day later. (Similar injections were also performed and analyzed at mid-embryogenesis in utero; see Materials and Methods). (*A*, *B*) Coronal section at the level of the optic chiasm in a wild-type newborn, stained with DAPI to label nuclei (*A*) and visualized under rhodamine fluorescence to display DiI-labeled axons (*B*). Axons transit through the optic chiasm normally. (*C*,*D*) Coronal section similar to *A* and *B* but in a *Vax1*$^{-/-}$ newborn. Axons fail to enter the brain at this level and terminate in an encapsulated, light-bulb-shaped knot; the optic chiasm is completely absent. (*E*,*F*) Coronal section, caudal to that of *A* and *B* at the level of the superior colliculus, in a wild-type newborn. Approximately 95% of labeled RGC axons cross to the opposite side of the brain at the chiasm and terminate in the contralateral superior colliculus (*F*), as is normal in the mouse. (*G*,*H*) Coronal section similar to *E* and *F* but in a *Vax1*$^{-/-}$ newborn. The rare axons that escape the knot in *D* project through lateral regions of the ventral hypothalamus that are normally Vax1 negative (see Fig. 2B), and terminate exclusively in the ipsilateral superior colliculus (*H*). Scale bars, 100 μm.

similar in histology to the capped light-bulb-like whorls of axons that develop at the base of the *Vax1* mutant hypothalamus. An equivalent failure in axon crossing at the hippocampal and anterior commissures, which are also normally apposed to populations of *Vax1*$^+$ cells at the midline, is also consistently observed in the *Vax1* mutants (Fig. 6D,F). In contrast, the commissures connecting the superior colliculi, which are caudal to the region of midline *Vax1* expression (Hallonet et al. 1998), are intact in these mutants (data not shown).

Essential features of midline axial patterning are preserved in Vax1$^{-/-}$ mice

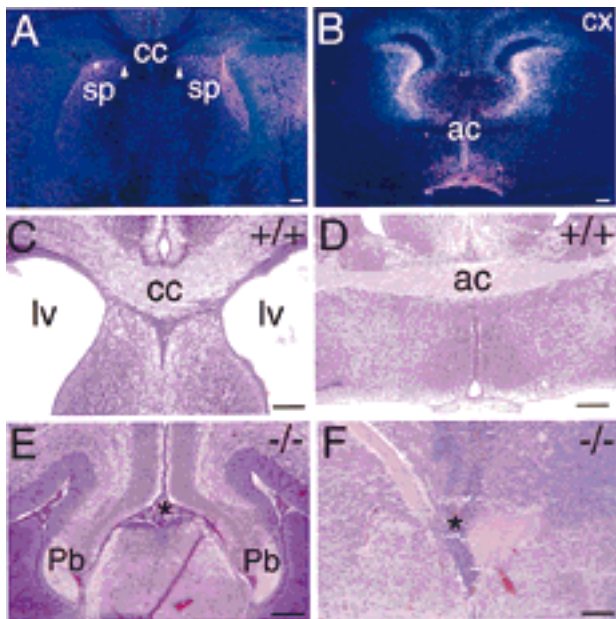What might account for the dramatic guidance defects seen in the optic nerve, optic chiasm, corpus callosum,

Figure 6. Anterior commissural fiber tracts fail to form in *Vax1* mutant mice. (*A*) High-power view of in situ hybridization in neonatal brain (coronal plane) showing that *Vax1* expression at the dorsal midline in the region of the septum (sp) and of the corpus callosum (cc) persists until birth. White arrowheads denote residual expression near the position of the midline glial sling of the embryo (Silver 1993). (*B*) Low-power view of a coronal section of an E16.5 mouse brain at the level of the anterior commissure (ac), showing *Vax1* expression in midline cells surrounding the commissural tract. Note the lack of *Vax1* mRNA in neurons of the developing cortex (cx). (*C*) Coronal section through the corpus callosum (cc) of a wild-type neonatal mouse brain. At this stage, most of the axons responsible for the interhemispheric connections have crossed the midline, and a thick bundle of axons (cc) crossing the midline is visualized by hematoxylin and eosin staining. Note the open lateral ventricles (lv). (*D*) Coronal section through a neonatal wild-type mouse brain at the level of the anterior commissure (ac), illustrating the normal midline crossing of axons in this commissure. (*E*) In *Vax1* mutants, the corpus callosum fails to form. No axons cross the midline but, instead, turn away into the lateral ventricles and accumulate in Probst-bundles (Pb)— thick knots of tangled axons adjacent to the dorsal midline. The point at which callosal axons would normally cross the midline is indicated by the asterisk. (*F*) Same plane of sectioning as in *D*, but in a *Vax1* mutant embryo in which axons fail to cross the midline in the anterior commissure. The normal midline crossing point is again indicated by the asterisk. Scale bars, 100 μm.

and hippocampal and anterior commissures of the *Vax1* mutants? It should first be noted that in each of these forebrain regions, the observed axon pathfinding defects are almost certainly cell nonautonomous. The neurons in the developing cortex, hippocampus, and olfactory bulbs whose axons normally course through commissural tracts (e.g., those whose axons make up the corpus callosum) do not express *Vax1* (Hallonet et al. 1998; Fig. 6A,B). Similarly, *Vax 1* expression stops abruptly at the optic disk and is not detected in the neuroepithelium that gives rise to the neural retina (Hallonet et al.

1998; Fig. 2A), in which RGC neurons, whose axons are misrouted in the optic nerve and are blocked from entering the brain, are born. Instead, the *Vax1* pathfinding defects appear to result from the loss of Vax1 from the midline cells with which axons and their growth cones normally interact.

As noted above, we have no evidence to support the hypothesis that the loss of Vax1 leads to the wholesale death of Vax1+ cells in any region of the forebrain. We also entertained the possibility that Vax1 might have a general structural role in patterning the ventral anterior midline. To address this possibility, we examined a battery of well-established cell fate and patterning markers that are expressed in the developing optic nerve, the rostral hypothalamus, and other Vax1+ regions at the midline (Marcus et al. 1999). These markers included the transcription factors *Pax2*, *Pax6*, *BF1*, *Dlx2*, *Nkx2.1*, and *Nkx2.2*, the chiasm markers RC2 and SSEA1, and the signaling protein Sonic Hedgehog (Shh).

We found that the *Vax1*−/− optic disk and stalk are normally patterned along both the dorsal–ventral and nasal–temporal axes during early RGC axonogenesis, as assessed by the expression of *Pax2* and *BF1* in the E10–E12 stalk and disk (Torres et al. 1996; Shimamura and Rubenstein 1997; Marcus et al. 1999). When the optic stalk first forms as an extension of the diencephalon, *Pax2* is initially expressed in its ventral but not dorsal aspect (Nornes et al. 1990), and this early dorsal–ventral patterning is maintained in the *Vax1* mutants (Fig. 7A). [By E12.5, all normal optic stalk cells are Pax2+ (Otteson et al. 1998).] Similarly, the transcription factor *BF1* is normally expressed in the nasal, but not the temporal, aspect of the early stalk, and this nasal–temporal gradient is also maintained in the mutants (Fig. 7B). We have observed that at later stages of embryonic development, a significant number of cells in the *Vax1* mutant optic nerve express *Pax6*, which is normally confined to the retina proper (Walther and Gruss 1991). These Pax6+ cells are first detected proximal to the developing retina (Fig. 8A), and later (by E14.5) frequently extend all the way to the brain (Fig. 8B). By this time, the developing mutant optic nerve contains both Pax2+ and Pax6+ cells (Fig. 8C,D). Although the presence of Pax6+ cells in the optic nerve might reflect a mispatterning event that proceeds in a lateral-to-medial graded fashion (beginning nearest the retina), we favor the alternative explanation that the unsealed hole at the back of the *Vax1* mutant eye (the coloboma) allows for the unimpeded migration of retinal cells into the nerve (Fig. 8E,F). This interpretation is supported by the fact that (1) both Pax6+ cells and retinal pigment epithelial cells are always initially detected in development closest to the retina itself, (2) the number of these cells in the distal mutant nerve (nearest the brain) increases with developmental age, and (3) in contrast to wild type, the *Vax1* mutant retina lacks a histologically apparent boundary with the optic nerve (Fig. 8E,F).

Consistent with the apparently normal axial patterning of the mutant optic stalk, we similarly found that nearly all of the markers of dorsal–ventral and anterior–
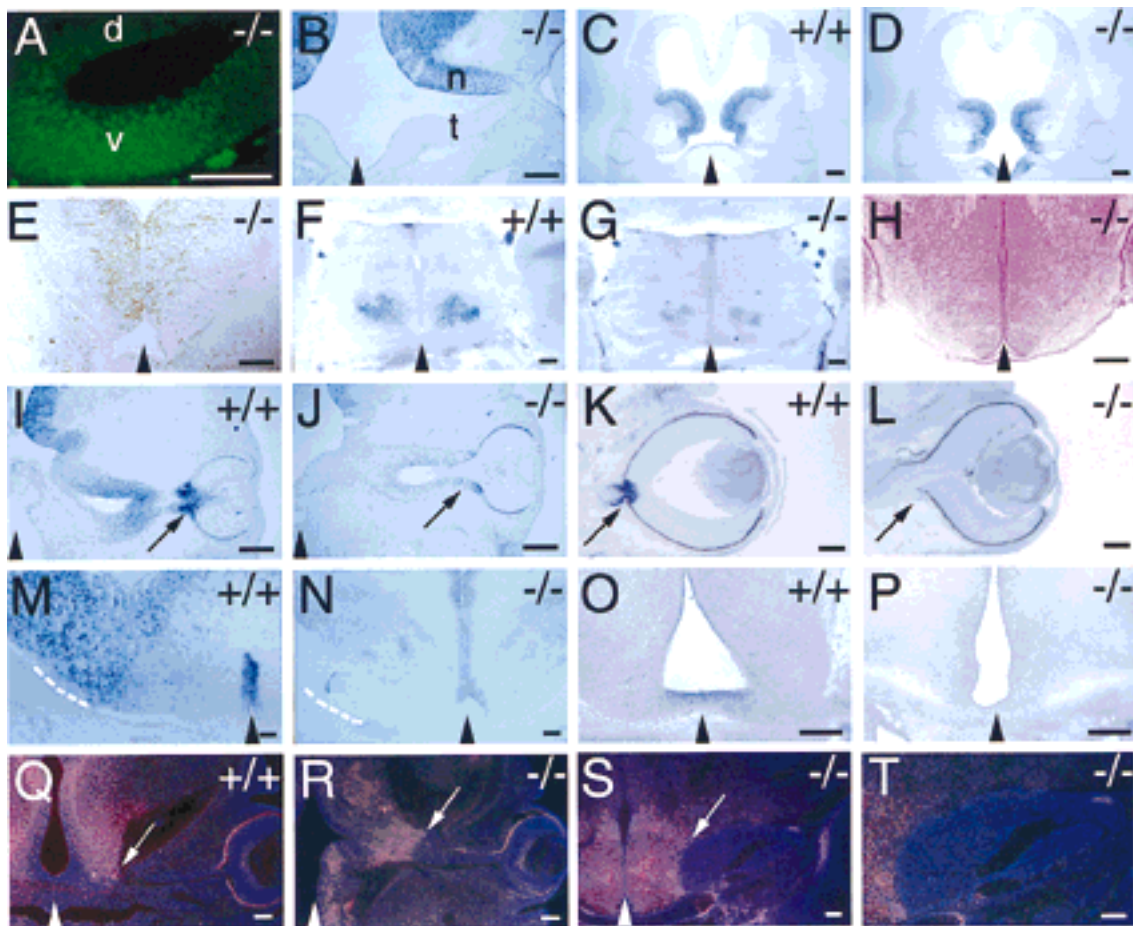
Figure 7. Cell fate and neural patterning in wild-type and *Vax1* mutant embryos. Black triangles at the bottom of selected panels indicate the position of the midline. (*A*) High-power view of the E11 optic stalk of a *Vax1* mutant (−/−), illustrating a normal distribution of *Pax2* expression in the ventral (v), but not dorsal (d), stalk. (*B*) Section of the E12 optic stalk of a *Vax1* mutant (eye at extreme right), illustrating a normal distribution of *BF1* expression in the nasal (n), but not temporal (t), stalk. (*C,D*) *Nkx2.1* expression in frontal sections of the ventral diencephalon (presumptive hypothalamus) of a wild-type (*C*, +/+) and *Vax1* mutant (*D*, −/−) mouse at E12. (*E*) RC2 expression in a frontal section of the hypothalamus of a *Vax1* mutant mouse at E13. Glial cells expressing the RC2 antigen are still present in a normal fashion in the mutant ventral diencephalon. (*F,G*) *Nkx2.2* expression in frontal sections of the hypothalamus of a wild-type (*F*, +/+) and a *Vax1* mutant (*G*, −/−) mouse at E19.5. (*H*) Coronal section of a E17.5 *Vax1* mutant ventral diencephalon stained with hematoxylin and eosin showing normal histology in the area of *Vax1* expression. (*I,J*) *Netrin-1* expression at the optic fissure and stalk of a wild-type (*I*, +/+) and *Vax1* mutant (*J*, −/−) mouse at E12 sectioned in a frontal orientation. Eyes are pointing to the right; arrows indicate the optic fissure, which fails to close in the mutant. Note marked reduction of *Netrin-1* in the mutant. (*K,L*) *Netrin-1* expression in the optic disk and proximal stalk of a wild-type (*K*, +/+) and *Vax1* mutant (*L*, −/−) mouse at E14.5. Note complete absence of *Netrin-1* in the mutant. Arrow in *K* points to the expression of *Netrin-1* in the closed optic disc, whereas the arrow in *L* indicates the lack of *Netrin-1* expression and the open fissure left at the eye/nerve boundary in the mutant embryos. (*M,N*) High-power view of *Netrin-1* expression in the hypothalamus of wild-type (*M*, +/+) and *Vax1* mutant (*N*, −/−) mouse at E18.5, shown in a coronal cut. Note that in *N*, *Netrin-1* expression in the lateral hypothalamus, at the entry point of the optic nerve (broken lines in *M* and *N*), is greatly reduced; surrounding the third ventricle, in which there is no overlap with *Vax1* expression, this *Netrin-1* expression is maintained. (*O,P*) *EphB3* receptor tyrosine kinase expression in wild-type (*O*, +/+) and *Vax1* mutant mouse (*P*, −/−) in the ventral diencephalon at E13.5, shown in a coronal section. Expression of *EphB3* is lost in the mutant embryo. (*Q,R*) Coronal sections of *Slit-1* mRNA expression, detected by radioactive in situ hybridization, in wild-type (*Q*, +/+) and *Vax1* mutant (*R*, −/−) mice at E13.5. Arrows indicate the optic nerve/hypothalamus boundary, which coincides with a pronounced border of *Slit-1* expression. Note that in *R*, this sharp *Slit-1* is maintained. (*S,T*) Medium power (*S*) and higher power (*T*) view of *Slit-1* expression, detected by radioactive in situ hybridization, in *Vax1* mutant mice (−/−) at E18.5. The *Slit-1* boundary barrier (arrowed in *S*) is maintained into late embryogenesis, at which point the capped bundle of RGC axons becomes directly wedged against it. Scale bars, 100 µm.

posterior axial patterning of the developing hypothalamus that we examined, including *Shh*, SSEA1, *Nkx2.1*, *Nkx2.2*, and RC2 are expressed in their normal, previously described domains, both early and late in embryogenesis, in the *Vax1* mutants. Representative examples for *Nkx2.1* and RC2 are shown in Figure 7C–E. The ex-
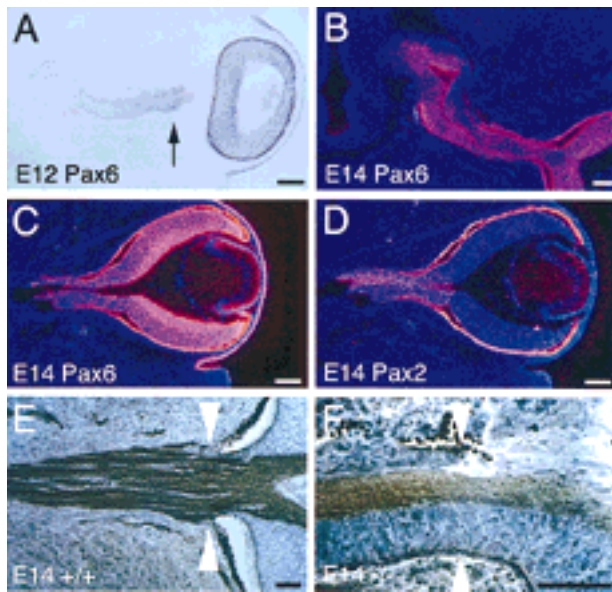
Figure 8. Pax6⁺ cells are ectopically present in the *Vax1⁻/⁻* optic nerve. (*A*) At E12, *Pax6* mRNA (visualized by digoxigenin in situ hybridization) is detected in the mutant neural retina, as expected, but also in the optic stalk, immediately adjacent to the retina (arrow). The remainder of the mutant stalk (nearer the brain) is Pax6⁻ at E12. (*B*) By E14, ectopic Pax6⁺ cells (detected by ³³P-labeled in situ hybridization) are present throughout the optic nerve. (*C,D*) In the E14 mutant optic nerve, both ectopic Pax6⁺ (*C*) and resident Pax2⁺ (*D*) cells are present. The sections in *C* and *D* are adjacent. (*E*) In the E14 wild-type embryo, a defined histological border (white arrowheads) is present between the eye and the optic nerve. Cells are stained with toluidine blue and axons immunostained with L1 antibody. (*F*) In E14 *Vax1* mutants, the eye/nerve border is missing (white arrowheads indicate the normal location). Note that there is a continuum of histologically indistinguishable cells from the retina into the nerve, and also that pigment epithelium, which does not express either *Vax1* or *Pax6*, streams into the nerve. Scale bars, 100 μm.

pression of two markers (*Shh, Nkx2.2*) appears to be subtly disordered and/or reduced in intensity by late embryogenesis in the *Vax1⁻/⁻* mice (Fig. 7F,G), but these effects may be in part accounted for by the lack of RGC axons at the optic chiasm. Their reduced expression notwithstanding, the boundaries of *Shh* and *Nkx2.2* expression are very similar to wild type (Fig. 7F,G). Finally, the *Vax1⁻/⁻* hypothalamus is largely indistinguishable from that of wild type in its general histology (Fig. 7H). Together, these data suggest that the basic patterning of the ventral midline of the anterior CNS is not grossly effected by the loss of Vax1.

Vax1 regulates expression of axon guidance cues

As noted above, axons at the anterior midline of the *Vax1* mutants grow as if they are repelled by populations of midline guidance cells to which they are normally attracted. This seeming conversion from attraction to repulsion led us to examine the expression of counterbalancing positive and negative axon guidance cues in *Vax1⁻/⁻* mice. This analysis yielded important insights into the axon pathfinding defects evident in the mutants. Perhaps the most significant alteration in the expression of a guidance cue that we observed is that for Netrin-1, an axon chemoattractant that is normally expressed by optic disk cells and stalk glial precursors, and to which RGC axons normally respond (Wang et al. 1996; de la Torre et al. 1997; Deiner et al. 1997). Expression of Netrin-1 by glial cells and their precursors in these structures is severely affected by the loss of Vax1 (Fig. 7I–L). As early as E12, *Netrin-1* mRNA is markedly reduced in the *Vax1⁻/⁻* optic disk and is nearly undetectable in the stalk (Fig. 7I,J), and by E14.5, this mRNA is no longer detectable in either structure (Fig. 7K,L). *Netrin-1* is similarly expressed in the Vax1⁺ region of rostral hypothalamus in which the optic nerve normally enters the brain, and this expression is also lost in the *Vax1* mutants (Fig. 7M,N). We have observed a similarly progressive loss of *Netrin-1* expression, from E12.5 to E14, from all of the normally Vax1⁺ cells that we have examined in these mice but not from cells that are normally Vax1⁻ (see Fig. 7N).

A second glial guidance cue that genetic experiments in the mouse have demonstrated to be important for axon guidance across the midline is the ephrin receptor EphB3, which, together with EphB2, is required for the formation of many of the same anterior commissural tracts (e.g., the corpus callosum) for which Vax1 is also essential (Orioli et al. 1996). In the forebrain, *EphB3* is expressed by many of the same midline cells that express *Vax1*, including those of the septum that are just ventral to the developing corpus callosum (Orioli et al. 1996; Fig. 6A). Interestingly, double knockouts of *EphB2/B3*, in addition to exhibiting *Vax1*-like commissural tract defects, also display a *Vax1*-like cleft palate. Consistent with these parallels, we find that *EphB3* expression at the midline of the hypothalamus is also exquisitely sensitive to the loss of *Vax1* at all midline positions that are normally Vax1⁺ (Fig. 7O,P). Like *Netrin-1*, *EphB3* is also expressed by cells that are not normally Vax1⁺, and *EphB3* expression is maintained in these cell populations in the *Vax1* mutants (data not shown).

Although loss of *Vax1* leads to the elimination of at least one attractive midline guidance cue, we find that the expression of the axon chemorepellent, Slit-1, is not affected in the hypothalamic midline of these mutants. Slit-1 appears to be particularly important for the regulation of axon pathfinding in this region of the CNS, because we have found that the border between the optic stalk/nerve and the ventral diencephalon (presumptive rostral hypothalamus) is delimited by a sharp boundary of *Slit-1* expression (Fig. 7Q,R). As axons cross from the nerve into the brain, their axons move from a *Slit-1⁻* to a strongly *Slit-1⁺* zone, which is also Vax1⁺ (Fig. 2B) and *Netrin-1⁺*. Whereas *Netrin-1* expression in this region is lost in the *Vax1* mutants (Fig. 7M,N), *Slit-1* expression is robustly maintained, and the dense whorl of RGC axons that eventually develops is wedged against the Slit-1⁺

cells at the midline of the mutant hypothalamus (Fig. 7S,T). Consistent with this pileup of RGC axons at the *Slit-1* expression boundary, RGC neurons have recently been found to express *Robo-2* (J. Braisted, T. Ringstedt, and D.D.M. O'Leary, unpubl.), one of two vertebrate homologs of the *Drosophila* Roundabout protein, which serves as the Slit receptor (Brose et al. 1999; Kidd et al. 1999; Li et al. 1999). Thus, for two regulators whose counterbalancing chemoattractive (Netrin) and chemorepellent (Slit) activities have been established both genetically and biochemically in *Drosophila*, the loss of Vax1 at the developing hypothalamic midline apparently shifts the balance of power in favor of chemorepulsion.

In vitro assay of axon guidance activity in Vax1$^{-/-}$ mice

To assess whether the observed immiscibility of axons and glia in the *Vax1* mutants might in fact reflect active chemorepulsion of the former by the latter, we performed a series of collagen gel experiments in which wild-type retinal explants were cocultured at a distance with optic stalk explants dissected from wild-type, heterozygous mutant, or homozygous mutant embryos at E11.5, E12.5, and E13.5 (see Materials and Methods). The results of these experiments are illustrated in Figure 9. We scored retinal axon outgrowth from a total of 75 cocultures after 4 days, and assigned the observed growth patterns to one of six categories—no axon outgrowth (ng in Fig. 9), growth strongly away from the optic stalk explant (–2), growth weakly away (–1), growth without preference (0), growth weakly toward (+1), and growth strongly toward (+2). Scoring was performed blind to genotypes. Our coculture results demonstrate a striking disparity between the axon guidance activities exhibited by wild-type and *Vax1*$^{-/-}$ optic stalk explants. A total of 56% (9/16) of retinal explants confronted with a wild-type optic stalk explant exhibited axon growth either weakly or strongly toward the explant, and none exhib-

ited growth strongly away (Fig. 9). In marked contrast, only 12% (2/16) of retinae confronted with a mutant stalk exhibited growth either weakly or strongly toward the explant, whereas 63% exhibited growth either strongly or weakly away (Fig. 9). Significantly, of the 16 retinae that were placed near *Vax1*$^{-/-}$ mutant stalk explants, 6 displayed growth strongly away from the explant. Note that the category distribution in Figure 9 is asymmetrically biased toward +2 for *Vax1*$^{+/+}$ explants, and toward –2 for *Vax1*$^{-/-}$ explants; it is centered around 0 for the *Vax1*$^{+/-}$ explants.

Discussion

Vax1 is crucial for axon guidance in the developing mouse forebrain

The results described above demonstrate that Vax1 is essential for the specification of axon trajectories in the developing mouse forebrain, particularly at and across the CNS midline. The inability of axons to interact productively with these midline regions is dramatically revealed by the failure of RGC axons to penetrate the brain at the ventral diencephalic midline and by the equivalent failure of axons that originate from neurons in the developing neocortex, hippocampus, and olfactory bulbs of the two cerebral hemispheres to cross the midline. As noted above, each of these failures occurs specifically at midline loci, either ventrally located (e.g., the presumptive hypothalamus) or more dorsally positioned (e.g., the septum apposed to the developing corpus callosum), which are populated by Vax1$^+$ cells. In all cases that we have examined, the neurons whose growth cones and axons are prevented from crossing the midline are Vax1$^-$, indicating that with respect to axon guidance defects, the effects of the *Vax1* mutation are cell nonautonomous.

The identity of the majority of the Vax1$^+$ guidance cells at the embryonic midline is, at this point, uncertain. Although they could be precursors to neurons or
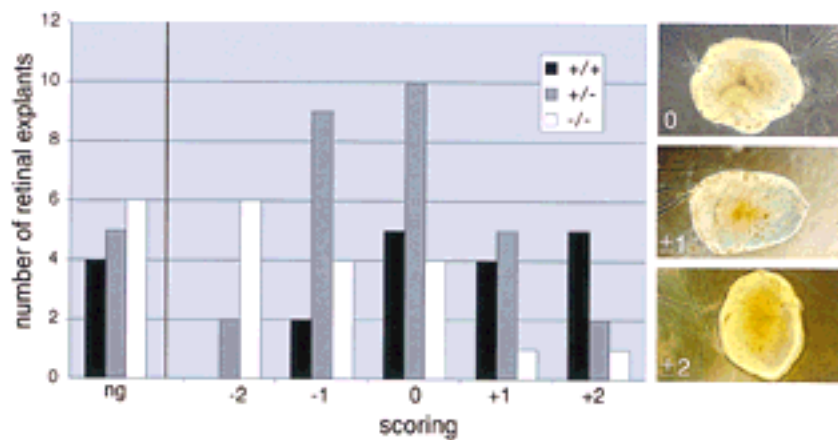

Figure 9. Collagen gel assay of retinal axon guidance by cells of wild-type and *Vax1* mutant optic stalk; qualitative scoring of results. Wild-type retinae were positioned close to embryonic optic stalk explants from wild-type (+/+, black bars), heterozygous (+/–, gray bars), or homozygous (–/–, white bars) *Vax1* mutant mice, and retinal axon outgrowth was scored after 4 days, as described in Materials and Methods. The histogram displays the number of retinal explants scored in six different categories: no growth (ng), strong away (–2), weak away (–1), unbiased (0), weak toward (+1), and strong toward (+2). Retinal axon outgrowth is biased away from homozygous mutant optic stalk explants (categories –2 and –1), whereas growth of these same axons is inversely biased toward wild-type optic stalks (+2 and +1). The outgrowth scores for the heterozygous explants exhibit an intermediate distribution. The three panels at *right* illustrate examples of retinal explants scored as unbiased (0), weakly biased (either toward or away) (±1), and strongly biased (±2).

glia, or both, our bias is that many or all of these cells will prove to be glial precursors. As noted above, this is clearly the case for the Vax1^{+} cells of the optic stalk. A definitive identification of the Vax1^{+} cells at the midline of the developing CNS will require the development of a specific Vax1 antibody and its use in single-cell double-labeling studies with midline glial markers.

Vax1 target genes and their role in axon guidance

We suggest that most or all of the axon guidance defects that result from the loss of Vax1 in midline cells are due to an attendant dysregulation of the genes encoding competing positive and negative guidance cues expressed in these midline cells. Our results demonstrate that one of these cues is Netrin-1, whose maintained expression at the midline of the early forebrain is clearly dependent on Vax1; by E14.5 in the *Vax1* mutants, *Netrin-1* expression can no longer be detected in the normally Vax1^{+} cells of the optic disk and stalk, the ventral diencephalon, and the midline cells abutting the forming anterior and hippocampal commissures and the corpus callosum. However, it is important to emphasize that whereas Vax1 may be essential for *Netrin-1* expression in these forebrain regions, this dependence does not extend throughout the rostral–caudal extent of the neuraxis. There is abundant *Netrin-1* expression in more caudal midline cells (e.g., those of the floor plate in the developing spinal cord) and in cells at the ventricular zone of the forebrain, which are Vax1^{−}, and these cells remain *Netrin-1*^{+} in the *Vax1* mutants.

This caveat notwithstanding, there are interesting parallels between the *Vax1* mutant phenotypes described above and the axon guidance defects reported for mouse *Netrin-1* mutants. These latter mutants are also acallosal and also lack both anterior and hippocampal commissures, and the histology of these malformations is largely indistinguishable from those seen in *Vax1*^{−/−} mice (Serafini et al. 1996). On some, but not all, genetic backgrounds, *Netrin-1* mutants variably exhibit an axon guidance phenotype at the optic disk in which RGC axons do not even enter the optic stalk (Deiner et al. 1997); this difference between the *Vax1* and *Netrin-1* mutants may be due to the fact that low levels of *Netrin-1* are still present in the E12 *Vax1*^{−/−} optic disk at the time that the first RGC axons enter the stalk (Fig. 7I,J). In addition to the similarities in the *Vax1* and *Netrin-1* mutant phenotypes, our observation of the frequent coexpression of the two genes, and our finding that loss of Vax1 leads to a rapid extinction of Netrin-1 expression throughout the normally Vax1^{+} areas of the mutant CNS but not to the death of Vax1^{+} cells suggest that the *Netrin-1* gene is an important target, either direct or indirect, of Vax1 action.

It should be noted, however, that this chemoattractant is likely to be only one of perhaps many guidance cues that are controlled by Vax1. Our results demonstrate that expression of the receptor tyrosine kinase EphB3 is lost in the *Vax1* mutants, specifically in those cells that are normally Vax1^{+}. Both Eph receptors and their ligands play important roles in axon guidance (O'Leary and Wilkinson 1999), and mutation of the mouse *EphB3* gene, in concert with the closely related *EphB2* gene, leads to a set of midline axon-crossing phenotypes that are partially overlapping with those exhibited by *Vax1* mutants (Orioli et al. 1996).

In the developing optic stalk and disk, the paired domain transcription factor Pax2 also appears to regulate *Netrin-1* expression. As noted above, mouse *Pax2* and zebrafish *Pax2.1* are expressed by cells that form the optic disk and by glial precursors and their descendants in the optic stalk and nerve (Torres et al. 1996; Macdonald et al. 1997). Importantly, null mutations in the genes encoding these proteins lead to coloboma and also to axon guidance defects in the optic stalk that are similar to those seen in the *Vax1* mutants; and in the zebrafish *Noi* mutant, the loss of *Pax2.1* similarly has been shown to lead to a pronounced reduction in *Netrin-1* expression in the developing optic stalk and nerve (Macdonald et al. 1997). Both Vax1 and Pax2 would therefore appear to be necessary for glial differentiation in the optic nerve, although neither is sufficient.

As described above, axons in the *Vax1* mutant forebrain appear to be repelled by the midline guidance cells with which they normally interact; axons and optic nerve glia are strictly segregated from one another in the mutant optic nerve despite their confined proximity, and axons that would normally form the corpus callosum and other interhemispheric commissures approach the midline but then fail to cross. This abject failure results in large whorls of tangled RGC axons at the base of the hypothalamus and in Probst bundles in place of a normal callosum. Although we suggest that the initial failure of growth cones to cross the midline at these loci is, for the most part, chemical in nature, it is very likely that the large encapsulated knots of axons that develop late in embryogenesis form a physical barrier to any subsequent commissural growth.

Our finding that a potent chemoattractant is lost from midline guidance cells at the same time that a potent chemorepellent is retained, suggests a straightforward hypothesis, namely, that the loss of Vax1 shifts the normally balanced presentation of attractive and repellent guidance cues at the anterior midline in favor of the latter. That is, axons now confront a sharp and discontinuous repulsive barrier at which the chemorepellent activities of molecules like Slit-1 are no longer modulated by the chemoattractant activities of cues such as Netrin-1. This hypothesis is strongly supported by the qualitative results of our collagen gel tests of retinal axon growth in response to confrontation with mutant versus wild-type optic stalk. In addition, it draws on compelling parallels to similar shifts in the balance of some of the same positive and negative midline cues that are seen in *Drosophila* mutants and is therefore one that we are currently pursuing in detail.

Materials and methods

Gene inactivation

The mouse *Vax1* gene was cloned from a strain 129SV genomic

library and was inactivated by deletion/replacement as diagrammed in Figure 1. The targeting vector was electroporated into W95 ES cells. Stable integrants were selected for using G418 (resistance to which is conferred by the *neo* cassette of Fig. 1), and nonhomologous integrants were selected against using FIAU (sensitivity to which is conferred by the thymidine kinase cassette of Fig. 1), both according to standard protocols (Tybulewicz et al. 1991). Four independent ES cell clones exhibiting homologous recombination of the targeting vector into the endogenous *Vax1* gene, as assessed by Southern blot with the 5′ external probe indicated in Figure 1, were injected into wild-type mouse blastocysts, which were in turn implanted into pseudopregnant foster mothers to generate high percentage chimeras, all by standard methods (Capecchi 1989). Mice analyzed in this report are 129SV × C57Bl/6 hybrid strains. Given the very restricted CNS expression of *Vax1*, we assessed loss of *Vax1* mRNA by in situ hybridization on sections cut through the hypothalamus of E13.5 mice, in which this is notably abundant. As a probe, we used a 540-bp *Bam*HI–*Pst*I fragment that spans part of the coding region, 330 bp of which is predicted to be present in any mRNA that might be expressed from the knockout alleles.

Expression studies

In situ hybridization reactions with the indicated riboprobes, either digoxygenin-labeled or ^{33}P-radiolabeled, were performed as described previously (Zhadanov et al. 1995; Braisted et al. 1997). The Pax2 antibody was from Zymed, the RC2 and SSEA1 antibodies were developed by M. Yamamoto, (Massachusetts General Hospital, Boston, MA) and D. Solter, (Max-Planck Institute of Immunology, Freiburg, Germany) respectively, and were obtained from the Developmental Studies Hybridoma Bank, and the L1 antibody was a gift of C. Lagenauer (Pittsburgh Medical School, PA).

Dissected mouse embryos were anesthetized and immersion fixed in 4%paraformaldehyde/PBS overnight at 4°C, followed by overnight infiltration with 20% sucrose. Cryoprotected tissues were then embedded in OCT medium (Miles) and cut with a cryostat at 20 µm. Tissues were then postfixed in 4% paraformaldehyde for 5 min followed by three 5-min washes in PBS.

Tissues were blocked with 10% normal goat serum/0.1%Triton X-100 (Sigma) at room temperature for 1 hr. Primary antibodies were applied overnight at 4°C (Pax2 antiserum diluted 1:400 and L1 antiserum 1:2000 in 0.1% normal goat serum/ 0.1% Triton-X100). For bright-field microscopy, sections were incubated for 1 hr with a biotinylated goat anti-rabbit secondary antibody and then for 30 min with an avidin–biotin–peroxidase complex (Vector Laboratories), followed by a 5 min reaction with enhanced DAB substrate (Boehringer Mannheim). Nuclei were counterstained lightly with toluidine blue, and sections were mounted with Permount (Fisher) and photographed. For fluorescence microscopy, immunolabeled sections were incubated for 1 hr at room temperature with an FITC-conjugated anti-rabbit secondary antibody (1:100, Jackson ImmunoResearch).

Axon tracing

All RGC axons of a single (right) eye were labeled by filling the retina with the fluorescent lipophilic dye DiI, as described previously (Simon and O'Leary 1992). Complete filling of the retina and labeling of RGC neurons across its full dorsal–ventral and nasal–temporal extents was confirmed by fluorescent examination of the retinae 24 hr after injection. Injections were performed both in utero at mid-embryogenesis (E16) and in new-

born pups. Injected embryos and newborns were allowed to develop for 24 hr after injection, either in utero (E17) or ex vivo (P1), at which time they were sacrificed, genotyped, perfused, and processed for analysis.

Collagen gel assay

Collagen gel assays were performed essentially as described previously (Sato et al. 1994). Briefly, retinae from E16 wild-type ICR mice were dissected and cut radially into eight pieces. Explants from optic stalks of wild-type, homozygous, and heterozygous *Vax1* mutant embryos were obtained from stages E11.5, E12.5, and E13.5. Explants of retinae and optic stalks were cocultured in three-dimensional rat tail collagen matrices (70 µl). Collagen was mixed with 10× minimal essential medium (MEM) at a 9:1 ratio; this mixture was cooled in ice, and sodium bicarbonate was added just prior to positioning the explants to promote gelling. Gelled substrates were overlaid with 500 µl of DMEM/F12 (GIBCO) supplemented with glutamine and 5% rat serum. Cultures were maintained up to 4 days at 37°C in a humidified incubator in an atmosphere of 7.5% CO_2. After completion of retinal axon outgrowth, collagen cocultures were fixed in 4% paraformaldehyde/0.1% glutaraldehyde and photographed with a phase-contrast microscope. Retinal outgrowth of all cocultures was scored qualitatively and binned into one of six different categories: no growth (ng), strong away (–2), weak away (–1), no directional bias (0), weak toward (+1), and strong toward (+2). A strong reaction of either polarity (± 2) was scored when >90% of the axons were clearly growing on one side, a weak reaction (± 1) was scored when 60%–90% of the axons were found on one side, and no bias was scored when the distribution on either side was 50%. All the scorings were done blind; the genotype of the optic stalk tissues was determined by Southern blot after the cultures were scored.

References

Anderson, M.G., G.L. Perkins, P. Chittick, R.J. Shrigley, and W.A. Johnson. 1995. *drifter*, a *Drosophila* POU-domain transcription factor, is required for correct differentiation and migration of tracheal cells and midline glia. *Genes & Dev.* **9:** 123–137.

Bartsch, U., F. Kirchhoff, and M. Schachner. 1989. Immunohistological localization of the adhesion molecules L1, N-CAM, and MAG in the developing and adult optic nerve of mice. *J. Comp. Neurol.* **284:** 451–462.

Battye, R., A. Stevens, and J.R. Jacobs. 1999. Axon repulsion

from the midline of the Drosophila CNS requires slit function. *Development* **126:** 2475–2481.

Braisted, J.E., T. McLaughlin, H.U. Wang, G.C. Friedman, D.J. Anderson, and D.D.M. O'Leary. 1997. Graded and lamina-specific distributions of ligands of EphB receptor tyrosine kinases in the developing retinotectal system. *Dev. Biol.* **191:** 14–28.

Brose, K., K.S. Bland, K.H. Wang, D. Arnott, W. Henzel, C.S. Goodman, M. Tessier-Lavigne, and T. Kidd. 1999. Slit proteins bind Robo receptors and have an evolutionarily conserved role in repulsive axon guidance. *Cell* **96:** 795–806.

Capecchi, M.R. 1989. Altering the genome by homologous recombination. *Science* **244:** 1288–1292.

Cunliffe, H.E., L.A. McNoe, T.A. Ward, K. Devriendt, H.G. Brunner, and M.R. Eccles. 1998. The prevalence of PAX2 mutations in patients with isolated colobomas or colobomas associated with urogenital anomalies. *J. Med. Genet.* **35:** 806–812.

Deiner, M.S., T.E. Kennedy, A. Fazeli, T. Serafini, M. Tessier-Lavigne, and D.W. Sretavan. 1997. Netrin-1 and DCC mediate axon guidance locally at the optic disc: Loss of function leads to optic nerve hypoplasia. *Neuron* **19:** 575–589.

de la Torre, J.R., V.H. Hopker, G.L. Ming, M.M. Poo, M. Tessier-Lavigne, A. Hemmati-Brivanlou, and C.E. Holt. 1997. Turning of retinal growth cones in netrin-1 gradient mediated by the netrin receptor DCC. *Neuron* **19:** 1211–1224.

Dressler, G.R., U. Deutsch, K. Chowdhury, H.O. Nornes, and P. Gruss. 1990. Pax2, a new murine paired-box-containing gene and its expression in the developing excretory system. *Development* **109:** 787–795.

Hallonet, M., T. Hollemann, R. Wehr, N.A. Jenkins, N.G. Copeland, T. Pieler, and P. Gruss. 1998. Vax1 is a novel homeobox-containing gene expressed in the developing anterior ventral forebrain. *Development* **125:** 2599–2610.

Hummel, T., T. Menne, H. Scholz, S. Granderath, K. Giesen, and C. Klambt. 1997. CNS midline development in Drosophila. *Perspect. Dev. Neurobiol.* **4:** 357–368.

Jacobs, J.R. and C.S. Goodman. 1989. Embryonic development of axon pathways in the Drosophila CNS. I. A glial scaffold appears before the first growth cones. *J Neurosci.* **9:** 2402–2241.

Kidd, T., K.S. Bland, and C.S. Goodman. 1999. Slit is the midline repellent for the robo receptor in Drosophila. *Cell* **96:** 785–794.

Klambt, C. 1993. The Drosophila gene pointed encodes two ETS-like proteins which are involved in the development of the midline glial cells. *Development* **117:** 163–176.

Klambt, C., J.R. Jacobs, and C.S. Goodman. 1991. The midline of the Drosophila central nervous system: A model for the genetic analysis of cell fate, cell migration, and growth cone guidance. *Cell* **64:** 801–815.

Li, H.S., J.H. Chen, W. Wu, T. Fagaly, L. Zhou, W. Yuan, S. Dupuis, Z.H. Jiang, W. Nash, C. Gick et al. 1999. Vertebrate slit, a secreted ligand for the transmembrane protein roundabout, is a repellent for olfactory bulb axons. *Cell* **96:** 807–818.

Livesey, F.J. and S.P. Hunt. 1997. Netrin and netrin receptor expression in the embryonic mammalian nervous system suggests roles in retinal, striatal, nigral, and cerebellar development. *Mol. Cell. Neurosci.* **8:** 417–429.

Macdonald, R., J. Scholes, U. Strahle, C. Brennan, N. Holder, M. Brand, and S.W. Wilson. 1997. The Pax protein Noi is required for commissural axon pathway formation in the rostral forebrain. *Development* **124:** 2397–2408.

Marcus, R.C. and C.A. Mason. 1995. The first retinal axon growth in the mouse optic chiasm: Axon patterning and the cellular environment. *J. Neurosci.* **15:** 6389–6402.

Marcus, R.C., R. Blazeski, P. Godement, and C.A. Mason. 1995. Retinal axon divergence in the optic chiasm: Uncrossed axons diverge from crossed axons within a midline glial specialization. *J. Neurosci.* **15:** 3716–3729.

Marcus, R.C., K. Shimamura, D. Sretavan, E. Lai, J.L. Rubenstein, and C.A. Mason. 1999. Domains of regulatory gene expression and the developing optic chiasm: Correspondence with retinal axon paths and candidate signaling cells. *J. Comp. Neurol.* **403:** 346–358.

Mason, C.A. and D.W. Sretavan. 1997. Glia, neurons, and axon pathfinding during optic chiasm development. *Curr. Opin. Neurobiol.* **7:** 647–653.

Mi, H. and B.A. Barres. 1999. Purification and characterization of astrocyte precursor cells in the developing rat optic nerve. *J. Neurosci.* **19:** 1049–1061.

Mitchell, K.J., J.L. Doyle, T. Serafini, T.E. Kennedy, M. Tessier-Lavigne, C.S. Goodman, and B.J. Dickson. 1996. Genetic analysis of Netrin genes in Drosophila: Netrins guide CNS commissural axons and peripheral motor axons. *Neuron* **17:** 203–215.

Nguyen Ba-Charvet, K.T., K. Brose, V. Marillat, T. Kidd, C.S. Goodman, M. Tessier-Lavigne, C. Sotelo, and A. Chedotal. 1999. Slit2-Mediated chemorepulsion and collapse of developing forebrain axons. *Neuron* **22:** 463–473.

Nornes, H.O., G.R. Dressler, E.W. Knapik, U. Deutsch, and P. Gruss. 1990. Spatially and temporally restricted expression of Pax2 during murine neurogenesis. *Development* **109:** 797–809.

O'Leary, D.D.M. and D.G. Wilkinson. 1999. Eph receptors and ephrins in neural development. *Curr. Opin. Neurobiol.* **9:** 65–73.

Ono, K., Y. Yasui, U. Rutishauser, and R.H. Miller. 1997. Focal ventricular origin and migration of oligodendrocyte precursors into the chick optic nerve. *Neuron* **19:** 283–292.

Orioli, D., M. Henkemeyer, G. Lemke, R. Klein, and T. Pawson. 1996. Sek4 and Nuk receptors cooperate in guidance of commissural axons and in palate formation. *EMBO J.* **15:** 6035–6049.

Otteson, D.C., E. Shelden, J.M. Jones, J. Kameoka, and P.F. Hitchcock. 1998. Pax2 expression and retinal morphogenesis in the normal and Krd mouse. *Dev. Biol.* **193:** 209–224.

Pfeffer, P.L., T. Gerster, K. Lun, M. Brand, and M. Busslinger. 1998. Characterization of three novel members of the zebrafish Pax2/5/8 family: Dependency of Pax5 and Pax8 expression on the Pax2.1 (noi) function. *Development* **125:** 3063–3074.

Probst, M. 1901. Über den Bau des balkenlosen Grosshirns, sowie über Mikrogyrie und Heterotypie der grauen Substanz. *Arch. Psychiatr.* **34:** 709–786.

Raff, M.C. 1989. Glial cell diversification in the rat optic nerve. *Science* **243:** 1450–1455.

Rothberg, J.M., J.R. Jacobs, C.S. Goodman, and S. Artavanis-Tsakonas. 1990. Slit: An extracellular protein necessary for development of midline glia and commissural axon pathways contains both EGF and LRR domains. *Genes & Dev.* **4:** 2169–2187.

Sanyanusin, P., L.A. Schimmenti, L.A. McNoe, T.A. Ward, M.E. Pierpont, M.J. Sullivan, W.B. Dobyns, and M.R. Eccles. 1995. Mutation of the PAX2 gene in a family with optic nerve colobomas, renal anomalies and vesicoureteral reflux. *Nat. Genet.* **9:** 358–364.

Sato, M., L. Lopez-Mascaraque, C.D. Heffner, and D.D.M. O'Leary. 1994. Action of a diffusible target-derived chemoattractant on cortical axon branch induction and directed growth. *Neuron* **13:** 791–803.

Serafini, T., S.A. Colamarino, E.D. Leonardo, H. Wang, R. Beddington, W.C. Skarnes, and M. Tessier-Lavigne. 1996. Netrin-1 is required for commissural axon guidance in the developing vertebrate nervous system. *Cell* **87:** 1001–1014.

Shimamura, K. and J.L. Rubenstein. 1997. Inductive interactions direct early regionalization of the mouse forebrain. *Development* **124:** 2709–2718.

Silver, J. 1993. Glia-neuron interactions at the midline of the developing mammalian brain and spinal cord. *Perspect. Dev. Neurobiol.* **1:** 227–236.

Silver, J. and M.Y. Ogawa. 1983. Postnatally induced formation of the corpus callosum in acallosal mice on glia-coated cellulose bridges. *Science* **220:** 1067–1069.

Silver, J., M.A. Edwards, and P.J. Levitt. 1993. Immunocytochemical demonstration of early appearing astroglial structures that form boundaries and pathways along axon tracts in the fetal brain. *J. Comp. Neurol.* **328:** 415–436.

Simon, D.K. and D.D.M. O'Leary. 1992. Development of topographic order in the mammalian retinocollicular projection. *J. Neurosci.* **12:** 1212–1232.

Small, R.K., P. Riddle, and M. Noble. 1987. Evidence for migration of oligodendrocyte–type-2 astrocyte progenitor cells into the developing rat optic nerve. *Nature* **328:** 155–157.

Soriano, N.S. and S. Russell. 1998. The Drosophila SOX-domain protein Dichaete is required for the development of the central nervous system midline. *Development* **125:** 3989–3996.

Tear, G., R. Harris, S. Sutaria, K. Kilomanski, C.S. Goodman, and M.A. Seeger. 1996. Commissureless controls growth cone guidance across the CNS midline in Drosophila and encodes a novel membrane protein. *Neuron* **16:** 501–514.

Torres, M., E. Gomez-Pardo, and P. Gruss. 1996. Pax2 contributes to inner ear patterning and optic nerve trajectory. *Development* **122:** 3381–3391.

Tybulewicz, V.L., C.E. Crawford, P.K. Jackson, R.T. Bronson, and R.C. Mulligan. 1991. Neonatal lethality and lymphopenia in mice with a homozygous disruption of the c-abl proto-oncogene. *Cell* **65:** 1153–1163.

Walther, C. and P. Gruss. 1991. Pax-6, a murine paired box gene, is expressed in the developing CNS. *Development* **113:** 1435–1449.

Wang, L.C., J. Dani, P. Godement, R.C. Marcus, and C.A. Mason. 1995. Crossed and uncrossed retinal axons respond differently to cells of the optic chiasm midline in vitro. *Neuron* **15:** 1349–1364.

Wang, L.C., R.A. Rachel, R.C. Marcus, and C.A. Mason. 1996. Chemosuppression of retinal axon growth by the mouse optic chiasm. *Neuron* **17:** 849–862.

Winberg, M.L., K.J. Mitchell, and C.S. Goodman. 1998. Genetic analysis of the mechanisms controlling target selection: Complementary and combinatorial functions of netrins, semaphorins, and IgCAMs. *Cell* **93:** 581–591.

Wu, W., K. Wong, J. Chen, Z. Jiang, S. Dupuis, J.Y. Wu, and Y. Rao. 1999. Directional guidance of neuronal migration in the olfactory system by the protein Slit. *Nature* **400:** 331–336.

Zhadanov, A.B., S. Bertuzzi, M. Taira, I.B. Dawid, and H. Westphal. 1995. Expression pattern of the murine LIM class homeobox gene Lhx3 in subsets of neural and neuroendocrine tissues. *Dev. Dyn.* **202:** 354–364.

Zinn, K. and Q. Sun. 1999. Slit branches out: A secreted protein mediates both attractive and repulsive axon guidance. *Cell* **97:** 1–4.